α-Al$_2$O$_3$-supported ZIF-8 SURMOF membranes: Diffusion mechanism of ethene/ethane mixtures and gas separation performance

Elvia P. Valadez Sánchez[a,*], Hartmut Gliemann[b], Katja Haas-Santo[a], Wenjin Ding[a], Edgar Hansjosten[a], Jonas Wohlgemuth[b], Christof Wöll[b], Roland Dittmeyer[a]

[a] *Institute for Micro Process Engineering (IMVT), Karlsruhe Institute of Technology, Hermann-von-Helmholtz-Platz 1, 76344, Eggenstein-Leopoldshafen, BW, Germany*
[b] *Institute of Functional Interfaces (IFG), Karlsruhe Institute of Technology, Hermann-von-Helmholtz-Platz 1, 76344, Eggenstein-Leopoldshafen, BW, Germany*

ABSTRACT

Keywords:
Liquid phase epitaxy
SURMOF
ZIF-8
Gas separation
Maxwell-Stefan

Metal-organic frameworks have been proven to offer the possibility of fabricating highly permeable and selective membranes. ZIF-8 is one of the most studied, attractive, and promising candidates given its known thermal stability and small pores connected by narrow sized windows of around 3.4 Å.

In this paper, liquid phase epitaxial (LPE) layer-by-layer (LBL) ZIF-8 SURMOF membranes were tested for gas separation of various binary feed mixtures of ethene/ethane (C$_2$H$_4$/C$_2$H$_6$) using the Wicke-Kallenbach technique. Permeation experiments of ethene or ethane in the presence of sweep gas were also conducted. A simulation program based on the generalized Maxwell-Stefan model was also used to analyze the separation performance of the SURMOF film in more detail. Its implementation consists in a discretization of the membrane, using then experimental and literature data in order to simulate the molar fluxes.

1. Introduction

The application of membrane technologies as an energetically favorable alternative for gas separation has been studied and developed over the last 30 years. Though great advances have been achieved, these technologies still exhibit challenges that must be studied and overcome in order to reach commercial feasibility [1–3].

Diverse types of membranes have been studied for gas separation so far. The known trade-off between membrane permeability and selectivity has been one of the key points behind the development and testing of new materials. Metal-organic frameworks (MOFs) are porous crystalline solid state materials composed of metal nodes and organic linkers that have been proven as capable to deliver simultaneously high permeabilities and selectivities, becoming a major material of study in this field [4]. This outstanding performance can be related to the high flexibility of MOFs in terms of geometry (e.g. pore sizes and shapes) and chemical properties when compared to other materials such as zeolites [5–7].

When speaking about the synthesis of MOFs for membrane applications, diverse techniques have been proposed in literature [8,9]. Nonetheless, the achievement of high quality defect-free MOF membranes is still highly challenging [10]. One of the possibilities to overcome common issues including cracks [11], pin-holes, and surface barriers [12] is liquid phase epitaxial (LPE) layer-by-layer (LBL) deposition. This approach consists in the sequential deposition of the metal precursors and organic linkers in the liquid phase [13] and can be performed by various procedures e.g., dipping [14], spraying [15], or spin-coating [16]. The excess reactants are removed by including a rinsing step with pure solvent in between the deposition steps. Previous to the deposition, the substrate must be activated chemically by the formation of self-assembled monolayers (SAMs) on the substrate interface. For instance, gold-coated substrates can be activated via thiols [17,18], while oxidic substrates can be treated with silanes [19,20]. This technique has been proven to deliver highly crystalline and oriented, monolithic surface-anchored metal-organic frameworks (SURMOFs) suitable for membrane application investigation [21–23].

Zeolitic imidazolate framework 8 (ZIF-8) is one of the mostly studied MOFs, greatly due to its known high thermal stability of up to 550 °C in a nitrogen atmosphere [24] and up to 200 °C under a relative humidity of 3% [25]. Its cubic structure consists of four- and six-membered rings enclosing a larger cavity of around 11 Å. Due to its pore size windows ranging around 3.4 Å, i.e. within several molecules' kinetic diameters, it has become an interesting candidate for gas separation, for instance of short-chain hydrocarbons [26–28].

In a previous work [29], the comparative growth of the ZIF-8 SURMOF on non-coated and gold-coated porous α-Al$_2$O$_3$ supports was

studied, concluding higher reproducibility, size homogeneity, and orientation of the ZIF-8 crystals on the latter. Here we report about the synthesis of further ZIF-8 SURMOF membranes, prepared by 175 deposition cycles using gold-coated porous α-Al$_2$O$_3$ supports. In the first section and as the first goal of this work, the performance of the synthesized membranes was studied. For that, gas separation experiments using the Wicke-Kallenbach technique for various feed binary mixtures of ethene/ethane at P_{abs} = 1.1 bar were performed. Additionally, gas permeation experiments of ethene or ethane in the presence of sweep gas were also conducted. The obtained experimental data was then combined with adsorption data extracted from literature [30] in order to calculate the single surface diffusivities of the studied components. In a second step, a simulation model was used to analyze the separation performance of the ZIF-8 SURMOF films in more detail. Adapted from the work by Ding [31–33], the simulation presented in this work focuses on the gas mixture (ethene/ethane) transport through the ZIF-8 SURMOF pores [34]. One of the important objectives is to understand the material's transport behavior as a base for an optimized design of the system for future applications. The simulation consisted in the discretization of the ZIF-8 layer modeled via the generalized Maxwell-Stefan model extended by Krishna, plus the consideration of the support's resistance [35,36]. To describe the chemical potential gradient, two different adsorption models were tested: Ideal adsorbed solution theory (IAST) and extended Langmuir (Ext. L.) [36,37].
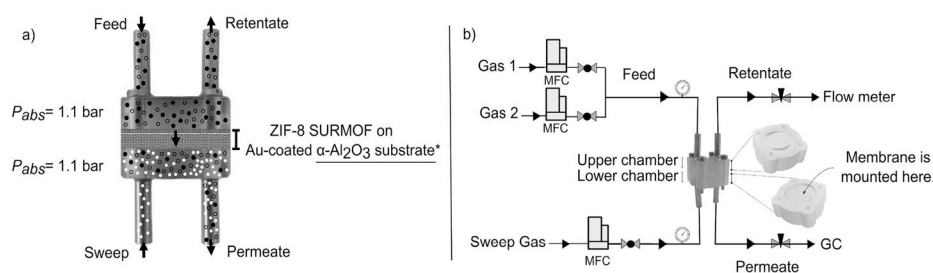
2. Experimental section

The ZIF-8 SURMOF membranes were synthesized according to previously published descriptions [29]. Further information regarding this point can be found in the Supporting Information. After the membranes were mounted inside the 3D-printed membrane modules, their overall quality was evaluated via hydrogen pressure-dependent experiments. Subsequently, the membranes were tested for single and binary feed gas mixtures. The complete experimental descriptions are presented in the next section.

2.1. Mounting of samples

The ZIF-8 SURMOF membranes were further analyzed using membrane modules printed with an Eden 260V 3D-printer (Stratasys) using VeroWhite and VeroClear PolyJet materials; the design of the modules ensures an even flow all over the membrane surface. The modules consist of an upper and lower chamber, each with an inlet for the feed or sweep flow, as well as with an outlet for the retentate or permeate flow as it is depicted in Fig. 1a. Each membrane was glued inside the lower chamber with the SURMOF layer facing upside. Both chambers were then assembled and sealed gas-tight using ELASTOSIL® M 4670 A/B (Wacker Chemie AG).

2.2. H$_2$ pressure-dependent experiments

To evaluate the overall quality of the membranes, the permeance of

hydrogen (N50, Air Liquide) as a function of increasing pressure was tested.

Hydrogen (150 ml·min^{-1}) was introduced through the feed side at different pressures (P_{abs} = 1.16–1.41 bar) while argon (Alphagaz 2, Air Liquide) (150 ml·min^{-1}) was used as the sweep gas and set to an initial P_{abs} = 1.1 bar. Once the system was in equilibrium, the retentate and permeate flow rates were measured using a bubble flow meter and a Definer 220 flow meter (Bios International Corporation).

2.3. Ethene/ethane (C$_2$H$_4$/C$_2$H$_6$) gas separation experiments

To perform the gas separation experiments, a set-up based on the Wicke-Kallenbach technique shown in Fig. 1b, was used. One of the advantages behind this technique concerns the elimination of forced flow [38].

Ethane (N35, Air Liquide) and ethene (N35, Air Liquide) were simultaneously introduced in the upper inlet (total flow: 60 ml·min^{-1}); helium (Alphagaz 1, Air Liquide) -sweep gas- was introduced in the lower inlet (60 ml·min^{-1}). Three different feed compositions were tested: equimolar (1:1), ethene-rich (2:1), and ethane-rich (1:2). The experiments were conducted at P_{abs} = 1.1 bar (equal on both chambers). The membrane was then left in operation until reaching stable conditions reflected by constant gas flow and constant concentration measurements in the retentate and permeate streams, respectively. These measurements were performed using a Definer 220 flow meter (Bios International Corporation) and a GC 7890B (Agilent Technologies) equipped with HP-Molesieve and HP-Plot Q columns (Agilent J&W GC Columns).

2.4. Single feed component permeation experiments

Using the same set-up as for the gas separation experiments, single feed gas permeation experiments were also conducted. Ethane or ethene was used as the feed gas (30 ml·min^{-1}), while helium was introduced as the sweep gas (30 ml·min^{-1}); the experiments were conducted at P_{abs} = 1.1 bar. Similar to the gas separation experiments, after reaching stabilization the gas flow and concentration were measured in the retentate and permeate streams, respectively.

3. Results and discussion

Four ZIF-8 SURMOF membrane samples were synthesized under the same conditions, characterized, and prior to any gas separation test, the hydrogen permeance through the membranes as a function of increasing pressure was verified. This test is performed in order to roughly evaluate the membrane's overall quality to exclude any significant influence of membrane pinholes or cracks on the gas permeation properties. Given the theoretical transport behavior considering ZIF-8's narrow sized windows of around 3.4 Å, hydrogen permeance must not change considerably during the experiment [39]. As it can be observed in the results reported in Fig. 2a, the permeances obtained indicate an overall good membrane quality with no large defects and/or

Fig. 1. a) Depiction of a 3D-printed membrane module (*supports bought from Fraunhofer IKTS; d = 13 mm, h = 1 mm, support d$_{50}$ = 2.5 µm, membrane d$_{50}$ = 70 nm, ε = 0.4–0.55), b) set-up sketch based on the Wicke-Kallenbach technique for gas separation experiments using a 3D-printed module composed of an upper and lower chamber containing the ZIF-8 SURMOF membrane.
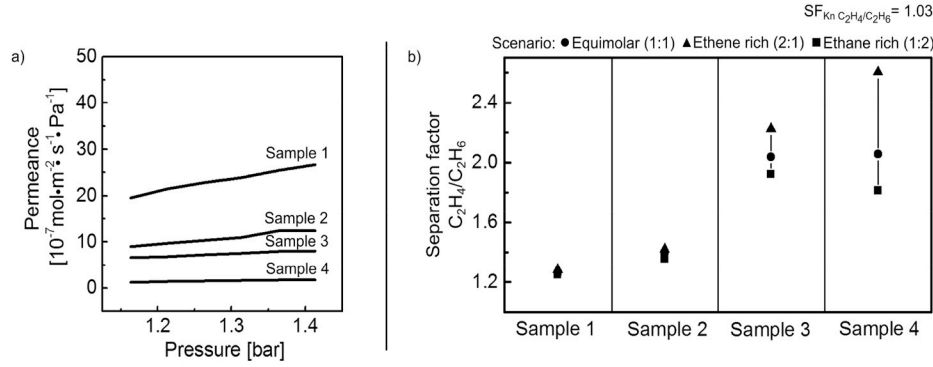
Fig. 2. a) Hydrogen permeance as a function of pressure through ZIF-8 SURMOF membranes, b) separation factors of samples 1 to 4 for different feed composition scenarios.

cracks, though a difference in permeance between them is observable. As reported in the supporting information, some of these variations can be attributed to the supports themselves. Nonetheless, the presence of micro-defects is also possible which could influence the performance of the membranes.

3.1. Ethene/ethane (C₂H₄/C₂H₆) gas separation

After the hydrogen permeance tests, gas separation experiments for ethene/ethane feed gas mixtures were conducted; the permeance of each gas was obtained and reported in Table 1.

The separation factor (SF) of the studied system was calculated with the following equation:

$$SF_{1,2} = \frac{y_1/y_2}{x_1/x_2} \tag{1}$$

where x and y correspond to the molar fractions of component 1 (ethene) and 2 (ethane) in the retentate and permeate streams respectively [40]. An SF = 1 represents therefore no separation. A SF ≠ 1 would instead reflect selectivity towards one of the components.

As shown in Fig. 2b, all of the membranes exhibited ethene selectivity. Nonetheless, samples 1 and 2 showed in general lower separation performance (SF ≈ 1.25–1.45) than samples 3 and 4 (SF ≈ 1.74–2.6) regardless of the feed composition scenario. This is in accordance with the hydrogen permeance experiments, in which samples 1 and 2 reported a slight increase in permeance with increasing pressures, suggesting the higher presence of micro-defects within the membrane surface. Furthermore, compared to sample 2, sample 1 shows a larger slope of the permeance with increasing hydrogen pressure, which goes along with a reduced selectivity. The presence of small defects in these membranes, though still exhibiting a slight selectivity towards ethene, favor non-selective transport delivering similar SFs regardless of the feed composition tested. Samples 3 and 4 on the other hand reported an almost constant permeance with increasing pressures, positively reflected in the ethene/ethane gas separation performance.

Furthermore, though the behavior of samples 3 and 4 are similar, the effect of the feed composition does play a significant role in the membranes' performance, especially for sample 4. This could be related to the association of lower hydrogen permeances with lower grain boundary micro-defects [14,41], resulting in a more significant enhancement or drop of the SFs. It is important to mention that the obtained SFs in the equimolar feed composition scenario for samples 3 and 4, which were prepared via the LPE LBL method (SFs ≈ 2.04) are comparable to published literature working with various synthesis techniques (SFs ≈ 2–2.6) [14,28,42,43]. Nonetheless as reported in multiple literature [42–44], due to the known preferential adsorption selectivity of the alkane competing with the preferential diffusion selectivity of the alkene, the application of ZIF-8 membranes in ethene/ethane separation is still quite limited and commercially attractive selectivities have not yet been reached.

3.2. Single feed component permeation experiments

Considering the previously obtained results, single feed gas permeation experiments were conducted on samples 3 and 4.

The surface diffusivity (D_i^s) for a component "i" is defined as:

$$D_i^s = -\frac{J_i^s}{\rho_m \cdot q_{sat} \cdot \nabla \theta_i} \cdot (1 - \overline{\theta}_i), \tag{2}$$

where J_i^s is the molar flux, $\overline{\theta}_i$ is the average surface coverage, $\nabla \theta_i$ is the gradient of the surface coverage in the direction of transport, ρ_m is the density of the framework extracted from literature [45], and q_{sat} is the saturation capacity [31]. The required adsorption data was extracted from literature [30] and fitted to the Langmuir model using the non-linear least-squares solver from MATLAB® in order to obtain k and q_{sat} (which are reported in the caption of Table 2). The coverages were then estimated using the Langmuir adsorption model [46]. The surface diffusivities for each gas and sample can be found in Table 2. These diffusivities and k and q_{sat} values were used in the simulation study reported in the next section.

3.3. Simulation study
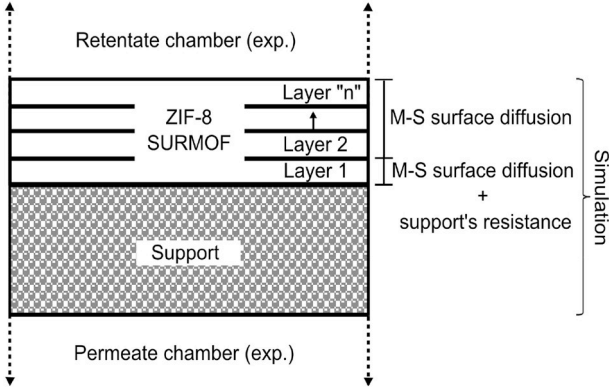
3.3.1. Implementation

In order to obtain a better insight of the studied system in this work, a simulation of the binary feed gas mixture through a ZIF-8 SURMOF membrane was implemented. The goal of the simulation, adapted from the work carried out by Ding [31–33], was the calculation of the simulated molar fluxes ($J_1^{s(sim)}$, $J_2^{s(sim)}$) where the components 1 and 2 represent ethene and ethane, respectively. The implementation consisted in the discretization of the ZIF-8 SURMOF film into "n" layers at which mass balances were conducted in order to describe the transport within the framework.

As depicted in Fig. 3, two complementary models were employed. For the ZIF-8 SURMOF layer, the generalized Maxwell-Stefan (M-S)

Table 1
Gas mixture permeances of ethene and ethane through various ZIF-8 SURMOF membranes for different ethene/ethane feed compositions.

Feed composition	Gas	Permeance Sample 1	Permeance Sample 2	Permeance Sample 3	Permeance Sample 4
		$[10^{-7} mol \cdot m^{-2} \cdot s^{-1} \cdot Pa^{-1}]$			
Equimolar	Ethene	6.99	2.85	1.59	0.43
	Ethane	5.21	1.98	0.76	0.21
Ethene rich (2:1)	Ethene	6.86	2.90	1.58	0.40
	Ethane	4.98	1.97	0.69	0.15
Ethane rich (1:2)	Ethene	6.92	2.77	1.52	0.37
	Ethane	5.19	1.98	0.77	0.20

Table 2
Calculated surface diffusivities (ethene and ethane) of samples 3 and 4 with $k_{ethene} = 0.167$ and $k_{ethane} = 0.215$ in $[bar^{-1}]$, $q_{sat_{ethene}} = 9.99$ and $q_{sat_{ethane}} = 14.39$ in $[mmol \cdot g^{-1}]$, $\rho_m = 924,250$ in $[g \cdot m^{-3}]$, $A_{mem} = 1.327 \cdot 10^{-4}$ in $[m^2]$, and $\delta_{mem} \approx 5 \cdot 10^{-7}$ in $[m]$.

	Component	J_i^s(single feed) [mmol·m^{-2}·s^{-1}]	$\nabla \theta_i$[m^{-1}]	$\bar{\theta}_i$	D_i^s [m^2·s^{-1}]	Ideal permselectivity
Sample 3	Ethene	11.72	−241194	0.0759	$4.86 \cdot 10^{-12}$	2.04
	Ethane	5.85	−307097	0.0879	$1.31 \cdot 10^{-12}$	
Sample 4	Ethene	3.92	−277801	0.0747	$1.42 \cdot 10^{-12}$	1.67
	Ethane	2.35	−343448	0.0900	$0.468 \cdot 10^{-12}$	

Fig. 3. Implementation sketch of the simulation study on a ZIF-8 SURMOF membrane.

surface diffusion model extended by Krishna was used [35]. This model has been generally proven to accurately describe binary gas systems considering three important points: the interactions between the adsorbed molecules, the interactions between the molecule and pore wall, and indirectly the adsorption fields [36,47],

$$-\frac{\theta_i}{RT}\nabla\mu_i = \sum_{\substack{j=1 \\ i \neq j}}^{2} \frac{\theta_j J_i^s - \theta_i J_j^s}{q_{sat} \cdot \rho_m \cdot D_{ij}^s} + \frac{J_i^s}{q_{sat} \cdot \rho_m \cdot D_i^s} \quad i,j = 1,2. \tag{3}$$

The cross-term diffusivity ($D_{12}^s = D_{21}^s$) was obtained using the empirical Vignes correlation [36,48] where 1 and 2 represent ethene and ethane, respectively:

$$D_{12}^s = D_1^{s\,\theta_1/(\theta_1+\theta_2)} D_2^{s\,\theta_2/(\theta_1+\theta_2)}. \tag{4}$$

Furthermore, the chemical potential gradient ($\nabla\mu_i$) can be linked to the surface coverage gradient by a matrix of thermodynamic factors, for which the selection of an adsorption model is required. In this simulation, the ideal adsorbed solution theory (IAST) and the extended Langmuir (Ext. L.) model were used alternatively [36,37].

Two simplifications concerning the above model were made. As mentioned before, the gas experiments presented in this work were conducted using the Wicke-Kallenbach method. One of the greatest disadvantages of this technique concerns the back permeation of the sweep gas into the retentate chamber thus affecting the permeation of the feed gases [49]. Nonetheless, such behavior has been reported in literature to influence every system differently, depending for instance on the nature of the sweep gas, feed composition, and temperature of operation [50]. For instance, in the experiments conducted in the hereby presented work ($P_{abs} = 1.1$ bar), negligible adsorption of helium in the ZIF-8 membranes can be assumed considering literature adsorption data [51]. Additionally, taking in mind that the gas permeation measurements in the hereby presented work were consistently performed using the Wicke-Kallenbach technique, it was assumed that the counter-flux –if present– existed in both permeation experiments performed and was thus already indirectly considered, i.e. the first simplifying assumption in the implemented simulation was that the counter-flux of helium could be neglected. Furthermore considering the different permeance values reported in Fig. 2, some differences even

within the best performing membranes were observable. As already mentioned in a previous section, some of these differences can be attributed to the supports themselves, but the presence of micro-defects is also possible. Nonetheless, the exact size of such micro-defects is unknown and the theoretical diffusion behavior through these defects is qualitatively similar (and therefore challenging to differentiate) [36]. Hence, as a second simplification, defects were not taken into account in the hereby simulation.

Referring again to Fig. 3, it can be further observed that the first ZIF-8 layer is in contact with the α-Al$_2$O$_3$ support. Therefore, in order to conduct the mass balance at this first ZIF-8 layer, the support's resistance must be also considered. Though no absolute pressure difference is present in the conducted experiments, a partial-pressure gradient does exist across the support. As reported in the work by van de Graaf and considering the similar support's properties and experimental conditions, this resistance was described as a result of molecular diffusion [36,50]:

$$-\frac{1}{RT}\nabla p_i = \sum_{j=1}^{3} \frac{y_j J_i - y_i J_j}{\varepsilon \cdot D_{ij}^{BF}} \quad i,j = 1,2,3. \tag{5}$$

where ε is the support's porosity (0.5) and D_{ij}^{BF} are the binary friction diffusivities for ethene (1), ethane (2), and the sweep gas, i.e. helium (3) calculated using the empirical correlation developed by Fuller, Schettler, and Giddings [52]. Though the three components were considered in the calculations, similar to the ZIF-8 layer, the counter-flux of helium was considered to be negligible (i.e. $J_3 = 0$). A linear profile was assumed from the interface of the ZIF-8 and support to the end of the support.

Finally, based on the simulated results, the simulated molar fluxes ($J_1^{s(sim)}$, $J_2^{s(sim)}$) were then estimated and compared to the experimental fluxes measured, in order to define the simulation's accuracy.

3.3.2. Results

Before proceeding with the simulation runs an important point was analyzed. As it might be recalled from the previous section, the single and binary feed gas experiments were conducted using the Wicke-Kallenbach technique which biggest disadvantage corresponds to the back permeation of the sweep gas into the retentate chamber. Since in this work, both single and binary feed gas experiments were conducted with the same technique, the effect –if present– was considered indirectly via the experimental data rather than explicitly in the simulation. To verify this point, the counter-flux was revised and determined to be present and actually around 10–15% higher in the single feed gas experiments resulting in underestimated diffusion coefficients. Additionally, as reported in literature, based on simulation studies these coefficients are not expected to vary greatly from single component to binary gas mixtures, nor between feed compositions at least in the pressure range used in this work [42]. In order to consider the above points, the surface diffusivities were manually tuned in the simulation for each membrane and composition scenario. An average value was then obtained as presented in Table 3. The table also contains the diffusivity ratios between ethene and ethane. The diffusivity of ethene is expected to be approximately 5 times higher than that of ethane in the ZIF-8 framework, particularly at low loadings [42]. The experimental and tuned surface diffusivities agree therefore with the expected ratios

Table 3

Experimental and average simulated (tuned) surface diffusivities of ethene and ethane for samples 3 and 4.

		M-S surface diffusivities [m² · s⁻¹]	
		Experimental	Simulated (Average)
Sample 3	Ethene	$4.86 \cdot 10^{-12}$	$9.75 \cdot 10^{-12}$
	Ethane	$1.31 \cdot 10^{-12}$	$2.29 \cdot 10^{-12}$
	Ratio	3.7	4.3
Sample 4	Ethene	$1.42 \cdot 10^{-12}$	$2.60 \cdot 10^{-12}$
	Ethane	$0.468 \cdot 10^{-12}$	$0.61 \cdot 10^{-12}$
	Ratio	3.0	4.3

and further support the initial underestimation of the diffusion coefficients.

Using these average values, the simulation was run for both adsorption models and different feed compositions (equimolar, ethene-rich, and ethane-rich feed) for samples 3 and 4. A number of n = 8 discretization layers were chosen in order to ensure that, even if non-linear profiles were presented, a good approximation could be reached; this point is further discussed at the end of this section. The results are reported in Table 4.

To explain the results obtained, several important known behaviors of the ZIF-8 framework must be introduced. When speaking about pure component adsorption, the difference between ethene and ethane is not significant; approx. 5–10% higher for ethane [42]. Nonetheless, once in a mixture state the behavior is known to considerably favor ethane adsorption. This is a common behavior observed in what have been called cation-free non-polar systems, i.e. a clear preferential adsorption of the alkane over the alkene is presented [42,53,54]. This has been associated to a cooperation/competition effect between adsorbed molecules of similar species as presented in the work by Do and Do [53]. The effect depends on feed composition and is also said to be intensified as the pore size decreases. Furthermore, the reason behind such behavior could be perhaps related to the molecular interactions between the methyl groups in ZIF-8 and ethane [54].

Based on the results presented in Table 4, the IAST adsorption model, as suggested in other literature [42], was able to accurately describe the transport through the ZIF-8 SURMOF framework. Furthermore, regardless of using the same surface diffusivity values for the different tested scenarios, the accuracy of the system was always below ± 10%, with the exception of the ethane flux simulation in the

ethene-rich scenario for sample 4. These values support that the diffusion coefficients don't vary greatly with feed composition. Finally, when comparing the results of samples 3 and 4, slightly lower accuracies were observed for sample 4. This behavior can be related to the intensification of the cooperation/competition effect at lower pore sizes, i.e. sample 4. Though the implemented simulation is able to accurately describe the transport of ethane and ethene through the ZIF-8 pores, it is not able to distinguish between different pore sizes, i.e. micro-defects, for which slight differences in accuracies can be distinguished between the tested samples.

Now referring to the extended Langmuir adsorption model results, the simulated molar fluxes were considerably overestimated. These results were not so surprising, for this model relies on single component adsorption data. As mentioned in previous paragraphs, the adsorption behavior of ethene and ethane is known to considerably vary between pure and mixed state. In order for this model to be thermodynamically consistent, the saturation capacities (q_{sat}) should be equal which is a known unrealistic condition, particularly in this binary feed system [55]. Still the extended Langmuir model has proven to be a simple model able to provide good insights into mixed gas adsorption in a lot of systems regardless of satisfying this assumption [56,57]. Nonetheless in this work, a description of ethene and ethane transport through the ZIF-8 pores with this adsorption model proved to be not completely appropriate due to the cooperation/competition effect proper of this and similar systems.

Finally based on the previous results, different numbers of discretization layers were tested using the IAST adsorption model. From the simulation data, the surface coverage as well as the molar fraction profiles were plotted exhibiting rather linear behaviors. This was further analyzed using the fitted adsorption data from literature [30], supporting that at the pressure used in this work, the coverages of ethene and ethane fall indeed within the linear section of their profiles. For this reason it was defined that 2 discretization layers are enough to accurately model both, the molar and surface coverage profiles through the ZIF-8 SURMOF membranes in this work. If a higher pressure were to be employed ($P_{abs} \geq 2.5$ bar), a greater number of discretization layers would be then required. Corresponding graphs can be found in the Supporting Information.

4. Conclusions and outlook

ZIF-8 SURMOF membranes were successfully synthesized using the

Table 4

Comparison of experimental and IAST and extended Langmuir simulated molar fluxes with their corresponding percent variation for different feed compositions (1 = ethene, 2 = ethane).

	Experimental data (binary gas mixture)			Simulated data		% variation	
	J_1^S	J_2^S	Adsorption Model	$J_1^{S(sim)}$	$J_2^{S(sim)}$	$\frac{J_1^{S(sim)}}{J_1^S} - 1$	$\frac{J_2^{S(sim)}}{J_2^S} - 1$
	[mmol·m⁻²·s⁻¹]			[mmol·m⁻²·s⁻¹]		%	
			Equimolar feed				
Sample 3	7.44	3.73	IAST	7.17	3.56	−4%	−5%
			Ext. L.	13.10	6.89	76%	85%
Sample 4	2.18	1.06	IAST	2.02	0.96	−7%	−9%
			Ext. L.	3.74	1.88	72%	77%
			Ethene-rich feed				
Sample 3	9.40	2.17	IAST	9.77	2.41	4%	11%
			Ext. L.	18.20	4.66	94%	115%
Sample 4	2.67	0.52	IAST	2.75	0.65	3%	25%
			Ext. L.	5.19	1.27	94%	144%
			Ethane-rich feed				
Sample 3	4.64	4.93	IAST	4.63	4.72	−0.2%	−4%
			Ext. L.	8.25	9.05	78%	84%
Sample 4	1.24	1.37	IAST	1.30	1.28	5%	−7%
			Ext. L.	2.36	2.48	90%	81%

liquid phase epitaxial layer-by-layer technique and tested for both single and binary feed gas separation of ethene and ethane. Regardless of their high degree of crystallinity and orientation, the membranes exhibited separation factors, $SF_{C_2H_4, C_2H_6}$, between 1.74 and 2.6 depending on the feed composition which is comparable to other published works, but still far away from commercial feasibility.

Using the obtained experimental data, the binary gas mixture transport of ethene and ethane through the ZIF-8 SURMOF membranes was simulated using the generalized Maxwell-Stefan surface diffusion model. The ZIF-8 SURMOF layer was discretized and the support's resistance was also considered. After comparing two different adsorption models, the implementation using the IAST adsorption model delivered the best simulation results for all scenarios and samples. As expected, gas mixture adsorption varied significantly from the pure component behavior, exhibiting a preferential adsorption of the alkane over the alkene. Furthermore, it could be also supported that the surface diffusivities for this system do not vary greatly with feed composition, at least at the pressure studied in this work.

For the sake of simplicity and seeking a general insight into the transport mechanism of the synthesized ZIF-8 SURMOF films, microdefects were neglected in this simulation study. Still, slight variations in the simulation results could be observed; in this case, the membrane exhibiting higher permeance delivered better accuracies. For this reason, future works should characterize and consider micro-defects to further improve the description of the system. Also, the surface diffusivities in the absence of sweep gas should be determined and the counter diffusion contribution in the system should be implemented in the simulation. The consideration of all these aspects in future related works will enhance our understanding of the transport through ZIF-8 membranes and the role defects might play on this and other MOF systems.

Acknowledgements

Abbreviations

Ext. L.	Extended Langmuir
IAST	Ideal adsorbed solution theory
LBL	Layer-by-layer
LPE	Liquid phase epitaxy
MFC	Mass flow controller
MOFs	Metal-organic frameworks
M-S	Maxwell-Stefan
SAM	Self-assembled monolayer
SF	Separation factor
SURMOF	Surface-anchored metal organic framework
ZIF	Zeolitic imidazolate framework

Nomenclature

y	Molar fraction in the permeate stream
x	Molar fraction in the retentate stream
ε	Support's porosity
A_{mem}	Area of membrane
D^s	M-S surface diffusivity
D_{ij}^s	M-S cross-term diffusivity
D_{ij}^{BF}	Binary friction diffusivity
J^s	Molar flux
$J^{s(sim)}$	Simulated molar flux
k	Adsorption constant
p_i	Partial pressure
ρ_m	Framework's density
q_{sat}	Saturation capacity
θ	Surface coverage
$\nabla\mu$	Chemical potential gradient
R	Universal gas constant
T	Temperature

References

[1] R. Faiz, K. Li, Olefin/paraffin separation using membrane based facilitated transport/chemical absorption techniques, Chem. Eng. Sci. 73 (2012) 261–284 https://doi.org/10.1016/j.ces.2012.01.037.

[2] A.F. Ismail, K.C. Khulbe, T. Matsuura, Gas Separation Membranes, Springer, Switzerland, 2015.

[3] R.W. Baker, B.T. Low, Gas separation membrane materials: a perspective, Macromolecules 47 (2014) 6999–7013 https://doi.org/10.1021/ma501488s.

[4] C. Zhang, Alkane and alkene separation by membrane operations, in: E. Drioli, L. Giorno (Eds.), Encyclopedia of Membranes, Springer, Berlin Heidelberg, 2016, pp. 55–56.

[5] J.-R. Li, J. Sculley, H.-C. Zhou, Metal–organic frameworks for separations, Chem. Rev. 112 (2011) 869–932 https://doi.org/10.1021/cr200190s.

[6] H.-C. Zhou, S. Kitagawa, Metal–organic frameworks (MOFs), Chem. Soc. Rev. 43 (2014) 5415–5418 https://doi.org/10.1039/C4CS90059F.

[7] J. Gascon, F. Kapteijn, B. Zornoza, V. Sebastián, C. Casado, J. Coronas, Practical approach to zeolitic membranes and coatings: state of the art, opportunities, barriers, and future perspectives, Chem. Mater. 24 (2012) 2829–2844 https://doi.org/10.1021/cm301435j.

[8] S. Qiu, M. Xue, G. Zhu, Metal–organic framework membranes: from synthesis to separation application, Chem. Soc. Rev. 43 (2014) 6116–6140 https://doi.org/10.1039/C4CS00159A.

[9] N. Stock, S. Biswas, Synthesis of metal-organic frameworks (MOFs): routes to various MOF topologies, morphologies, and composites, Chem. Rev. 112 (2011) 933–969 https://doi.org/10.1021/cr200304e.

[10] M. Shah, M.C. McCarthy, S. Sachdeva, A.K. Lee, H.-K. Jeong, Current status of metal–organic framework membranes for gas separations: promises and challenges, Ind. Eng. Chem. Res. 51 (2012) 2179–2199 https://doi.org/10.1021/ie202038m.

[11] E. Adatoz, A.K. Avci, S. Keskin, Opportunities and challenges of MOF-based membranes in gas separations, Separ. Purif. Technol. 152 (2015) 207–237 https://doi.org/10.1016/j.seppur.2015.08.020.

[12] L. Heinke, Z. Gu, C. Wöll, The surface barrier phenomenon at the loading of metal-organic frameworks, Nat. Commun. 5 (2014), https://doi.org/10.1038/ncomms5562.

[13] O. Shekhah, J. Liu, R. Fischer, C. Wöll, MOF thin films: existing and future applications, Chem. Soc. Rev. 40 (2011) 1081–1106 https://doi.org/10.1039/C0CS00147C.

[14] O. Shekhah, R. Swaidan, Y. Belmabkhout, M. Du Plessis, T. Jacobs, L.J. Barbour, I. Pinnau, M. Eddaoudi, The liquid phase epitaxy approach for the successful construction of ultra-thin and defect-free ZIF-8 membranes: pure and mixed gas transport study, Chem. Commun. 50 (2014) 2089–2092 https://doi.org/10.1039/C3CC47495J.

[15] H.K. Arslan, O. Shekhah, J. Wohlgemuth, M. Franzreb, R.A. Fischer, C. Wöll, High-throughput fabrication of uniform and homogenous MOF coatings, Adv. Funct. Mater. 21 (2011) 4228–4231 https://doi.org/10.1002/adfm.201101592.

[16] V. Chernikova, O. Shekhah, M. Eddaoudi, Advanced fabrication method for the preparation of MOF thin films: liquid-phase epitaxy approach meets spin coating method, ACS Appl. Mater. Interfaces 8 (2016) 20459–20464 https://doi.org/10.1021/acsami.6b04701.

[17] A. Ulman, Formation and structure of self-assembled monolayers, Chem. Rev. 96 (1996) 1533–1554 https://doi.org/10.1021/cr9502357.

[18] C.D. Bain, E.B. Troughton, Y.T. Tao, J. Evall, G.M. Whitesides, R.G. Nuzzo, Formation of monolayer films by the spontaneous assembly of organic thiols from solution onto gold, J. Am. Chem. Soc. 111 (1989) 321–335 https://doi.org/10.1021/ja00183a049.

[19] J. Sagiv, Organized monolayers by adsorption. 1. Formation and structure of oleophobic mixed monolayers on solid surfaces, J. Am. Chem. Soc. 102 (1980) 92–98 https://doi.org/10.1021/ja00521a016.

[20] R. Maoz, L. Netzer, J. Gun, J. Sagiv, Self-assembling monolayers in the construction of planned supramolecular suctures and as modifiers of surface properties, J. Chim. Phys. 85 (1988) 1059–1065 https://doi.org/10.1051/jcp/1988851059.

[21] O. Shekhah, H. Wang, S. Kowarik, F. Schreiber, M. Paulus, M. Tolan, C. Sternemann, F. Evers, D. Zacher, R.A. Fischer, C. Wöll, Step-by-step route for the synthesis of metal − organic frameworks, J. Am. Chem. Soc. 129 (2007)

15118–15119 https://doi.org/10.1021/ja076210u.

[22] O. Shekhah, Layer-by-layer method for the synthesis and growth of surface mounted metal-organic frameworks (SURMOFs), Materials 3 (2010) 1302–1315 https://doi.org/10.3390/ma3021302.

[23] H. Gliemann, C. Wöll, Epitaxially grown metal-organic frameworks, Mater. Today 15 (2012) 110–116 https://doi.org/10.1016/S1369-7021(12)70046-9.

[24] K.S. Park, Z. Ni, A.P. Côté, J.Y. Choi, R. Huang, F.J. Uribe-Romo, H.K. Chae, M. O'Keeffe, O.M. Yaghi, Exceptional chemical and thermal stability of zeolitic imidazolate frameworks, Proc. Natl. Acad. Sci. 103 (2006) 10186–10191 https://doi.org/10.1073/pnas.0602439103.

[25] J. Caro, Are MOF membranes better in gas separation than those made of zeolites? Curr. Opin. Chem. Eng. 1 (2011) 77–83 https://doi.org/10.1016/j.coche.2011.08.007.

[26] H.B. Park, J. Kamcev, L.M. Robeson, M. Elimelech, B.D. Freeman, Maximizing the right stuff: the trade-off between membrane permeability and selectivity, Science (2017) 356 eaab0530 https://doi.org/10.1126/science.aab0530.

[27] V.M.A. Melgar, J. Kim, M.R. Othman, Zeolitic imidazolate framework membranes for gas separation: a review of synthesis methods and gas separation performance, J. Ind. Eng. Chem. 28 (2015) 1–15 https://doi.org/10.1016/j.jiec.2015.03.006.

[28] Y. Pan, Z. Lai, Sharp separation of C2/C3 hydrocarbon mixtures by zeolitic imidazolate framework-8 (ZIF-8) membranes synthesized in aqueous solutions, Chem. Commun. 47 (2011) 10275–10277 https://doi.org/10.1039/C1CC14051E.

[29] E.P. Valadez Sánchez, H. Gliemann, K. Haas-Santo, C. Wöll, R. Dittmeyer, ZIF-8 SURMOF membranes synthesized by Au-assisted liquid phase epitaxy for application in gas separation, Chem. Ing. Tech. 88 (2016) 1798–1805 https://doi.org/10.1002/cite.201600061.

[30] U. Böhme, B. Barth, C. Paula, A. Kuhnt, W. Schwieger, A. Mundstock, J. Caro, M. Hartmann, Ethene/ethane and propene/propane separation via the olefin and paraffin selective metal–organic framework adsorbents CPO-27 and ZIF-8, Langmuir 29 (2013) 8592–8600 https://doi.org/10.1021/la401471g.

[31] W. Ding, Simulation-Assisted Design of Polycrystalline Zeolite Catalysts, KIT Scientific Publishing, Karlsruhe, 2016.

[32] W. Ding, H. Li, P. Pfeifer, R. Dittmeyer, Crystallite-pore network model of transport and reaction of multicomponent gas mixtures in polycrystalline microporous media, Chem. Eng. J. 254 (2014) 545–558 https://doi.org/10.1016/j.cej.2014.05.081.

[33] W. Ding, M. Klumpp, S. Lee, S. Reuß, S.A. Al-Thabaiti, P. Pfeifer, W. Schwieger, R. Dittmeyer, Simulation of one-stage dimethyl ether synthesis over a core-shell catalyst, Chem. Ing. Tech. 87 (2015) 702–712 https://doi.org/10.1002/cite.201400157.

[34] E.P. Valadez Sánchez, Thin Film MOFs (SURMOFs) for Application in Gas Separation, KIT Scientific Publishing, Karlsruhe, 2019.

[35] R. Krishna, Multicomponent surface diffusion of adsorbed species: a description based on the generalized Maxwell—stefan equations, Chem. Eng. Sci. 45 (1990) 1779–1791 https://doi.org/10.1016/0009-2509(90)87055-W.

[36] J.M. van de Graaf, F. Kapteijn, J.A. Moulijn, Modeling permeation of binary mixtures through zeolite membranes, AIChE J. 45 (1999) 497–511 https://doi.org/10.1002/aic.690450307.

[37] A. Myers, J.M. Prausnitz, Thermodynamics of mixed-gas adsorption, AIChE J. 11 (1965) 121–127 https://doi.org/10.1002/aic.690110125.

[38] J. Kärger, D.M. Ruthven, D.N. Theodorou, Diffusion in Nanoporous Materials, Wiley-VCH Verlag GmbH & Co. KGaA, Germany, 2012.

[39] D. Farrusseng, Metal-organic Frameworks: Applications from Catalysis to Gas Storage, Wiley-VCH Verlag GmbH & Co. KGaA, Singapore, 2011.

[40] W.F. Guo, T.-S. Chung, T. Matsuura, Pervaporation study on the dehydration of aqueous butanol solutions: a comparison of flux vs. permeance, separation factor vs. selectivity, J. Membr. Sci. 245 (2004) 199–210 https://doi.org/10.1016/j.memsci.2004.07.025.

[41] J. Yao, H. Wang, Zeolitic imidazolate framework composite membranes and thin films: synthesis and applications, Chem. Soc. Rev. 43 (2014) 4470–4493 https://doi.org/10.1039/C3CS60480B.

[42] H. Bux, C. Chmelik, R. Krishna, J. Caro, Ethene/ethane separation by the MOF membrane ZIF-8: molecular correlation of permeation, adsorption, diffusion, J. Membr. Sci. 369 (2011) 284–289 https://doi.org/10.1016/j.memsci.2010.12.001.

[43] J.B. James, J. Wang, L. Meng, Y. Lin, ZIF-8 membrane ethylene/ethane transport characteristics in single and binary gas mixtures, Ind. Eng. Chem. Res. 56 (2017) 7567–7575 https://doi.org/10.1021/acs.iecr.7b01536.

[44] M. Rungta, C. Zhang, W.J. Koros, L. Xu, Membrane-based ethylene/ethane separation: the upper bound and beyond, AIChE J. 59 (2013) 3475–3489 https://doi.org/10.1002/aic.14105.

[45] R. Krishna, J.M. van Baten, Hydrogen bonding effects in adsorption of water–alcohol mixtures in zeolites and the consequences for the characteristics of the Maxwell–Stefan diffusivities, Langmuir 26 (2010) 10854–10867 https://doi.org/10.1021/la100737c.

[46] J. Toth, Adsorption, CRC Press, 2002.

[47] S.K. Bhatia, M.R. Bonilla, D. Nicholson, Molecular transport in nanopores: a theoretical perspective, Phys. Chem. Chem. Phys. 13 (2011) 15350–15383 https://doi.org/10.1039/C1CP21166H.

[48] A. Vignes, Diffusion in binary solutions. Variation of diffusion coefficient with composition, Ind. Eng. Chem. Fundam. 5 (1966) 189–199 https://doi.org/10.1021/i160018a007.

[49] A.K. Pabby, S.S. Rizvi, A.M.S. Requena, Handbook of Membrane Separations: Chemical, Pharmaceutical, Food, and Biotechnological Applications, CRC press, 2015.

[50] J.M. van de Graaf, F. Kapteijn, J.A. Moulijn, Methodological and operational aspects of permeation measurements on silicalite-1 membranes, J. Membr. Sci. 144 (1998) 87–104 https://doi.org/10.1016/S0376-7388(98)00032-5.

[51] C. Zhang, R.P. Lively, K. Zhang, J.R. Johnson, O. Karvan, W.J. Koros, Unexpected molecular sieving properties of zeolitic imidazolate framework-8, J. Phys. Chem. Lett. 3 (2012) 2130–2134 https://doi.org/10.1021/jz300855a.

[52] E.N. Fuller, P.D. Schettler, J.C. Giddings, New method for prediction of binary gas-phase diffusion coefficients, Ind. Eng. Chem. 58 (1966) 18–27 https://doi.org/10.1021/ie50677a007.

[53] D. Do, H. Do, Cooperative and competitive adsorption of ethylene, ethane, nitrogen and argon on graphitized carbon black and in slit pores, Adsorption 11 (2005) 35–50 https://doi.org/10.1007/s10450-005-1091-y.

[54] M.C. Kroon, L.F. Vega, Selective paraffin removal from ethane/ethylene mixtures by adsorption into aluminum methylphosphonate-α: a molecular simulation study, Langmuir 25 (2009) 2148–2152 https://doi.org/10.1021/la803042z.

[55] A. Ahmadpour, K. Wang, D. Do, Comparison of models on the prediction of binary equilibrium data of activated carbons, AIChE J. 44 (1998) 740–752 https://doi.org/10.1002/aic.690440322.

[56] A. Kapoor, J. Ritter, R.T. Yang, An extended Langmuir model for adsorption of gas mixtures on heterogeneous surfaces, Langmuir 6 (1990) 660–664 https://doi.org/10.1021/la00093a022.

[57] R.T. Yang, Gas Separation by Adsorption Processes, Butterworth Publishers, United States of America, 1987.